Aneasy and sensitive sandwich assay for detection of Mycobacterium tuberculosis Ag85B antigen using quantum dots and gold nanorods

Eun Ju Kim, Eun Bee Kim, Seung Woo Lee, Seon Ah Cheon, Hwa-Jung Kim, Jaebeom Lee, Mi-Kyung Lee, Sungho Ko, Tae Jung Park

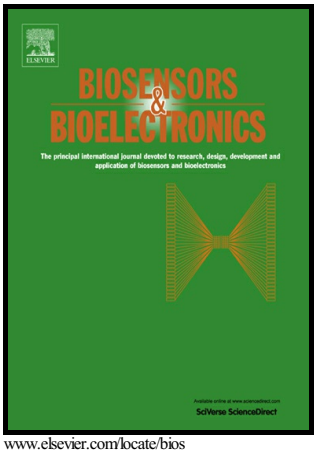

www.elsevier.com/locate/bios

PII: S0956-5663(16)30790-4
DOI: http://dx.doi.org/10.1016/j.bios.2016.08.034
Reference: BIOS9031

To appear in: *Biosensors and Bioelectronic*

Received date: 6 June 2016
Revised date: 5 August 2016
Accepted date: 11 August 2016

Cite this article as: Eun Ju Kim, Eun Bee Kim, Seung Woo Lee, Seon Ah Cheon Hwa-Jung Kim, Jaebeom Lee, Mi-Kyung Lee, Sungho Ko and Tae Jung Park Aneasy and sensitive sandwich assay for detection of Mycobacterium tuberculosis Ag85B antigen using quantum dots and gold nanorods, *Biosensor and Bioelectronic,* http://dx.doi.org/10.1016/j.bios.2016.08.034

An easy and sensitive sandwich assay for detection of *Mycobacterium tuberculosis* Ag85B antigen using quantum dots and gold nanorods

Eun Ju Kim[a], Eun Bee Kim[a], Seung Woo Lee[a], Seon Ah Cheon[a], Hwa-Jung Kim[b], Jaebeom Lee[c], Mi-Kyung Lee[d], Sungho Ko[e]*, and Tae Jung Park[a]*

[a]Department of Chemistry, Chung-Ang University, 84 Heukseok-ro, Dongjak-gu, Seoul 06974, Republic of Korea

[b]Department of Microbiology and Research Institute for Medical Science, College of Medicine, Chungnam National University, Daejeon 301-747, Republic of Korea

[c]Departments of Nano Fusion and Cogno-Mechatronics Engineering, Pusan National University, Busan 609-735, Republic of Korea

[d]Department of Laboratory Medicine, Chung-Ang University Hospital, 84 Heukseok-ro, Dongjak-gu, Seoul 06974, Republic of Korea

[e]Department of Biotechnology, CHA University, 335 CHA Bio Complexes, Pangyo-ro, Bundang-gu, Seongnam, Gyeongghi-do 463-836, Republic of Korea

shko7@cha.ac.kr (S.K.)

tjpark@cau.ac.kr (T.J.P.)

*Corresponding authors. Tel: +82-2-820-5220; fax: +82-2-825-4736.

ABSTRACT

Mycobacterium tuberculosis is a serious global infectious pathogen causing tuberculosis (TB). The development of an easy and sensitive method for the detection of *M. tuberculosis* is in urgent need due to complex and low specificity of the current assays. Herein, we present a novel method for *M. tuberculosis* detection based on a sandwich assay via antigen-antibody

interaction using silica-coated quantum dots (SiQDs) and gold nanorods (AuNRs). A genetically engineered recombinant antibody (GBP-50B14 and SiBP-8B3) was bound to surfaces of AuNRs and SiQDs respectively, without any surface modification. The antigen-antibody interaction was revealed using *M. tuberculosis*-specific secretory antigen, Ag85B. Two biocomplexes showed a quenching effect in the presence of the target antigen through a sandwich assay. The assay response was in the range of 1×10^{-3} – 1×10^{-10} μg mL^{-1} (R = 0.969) and the limit of detection for Ag85B was 13.0 pg mL^{-1}. The Ag85B was selectively detected using three different proteins (CFP10, and BSA), and further specifically confirmed by the use of spiked samples. Compared with existing methods, a highly sensitive and selective method for Ag85B-expressing *M. tuberculosis* detection has been developed for better diagnosis of TB.

Keywords: Mycobacterium tuberculosis; Ag85B; biosensor; gold nanorods; quantum dots.

1. Introduction

Mycobacterium tuberculosis, the main causative agent of tuberculosis (TB), is responsible for more deaths per year than any other bacterial pathogen. According to the World Health Organization (WHO, Global *Tuberculosis* Control Report, 2014), about 9.6 million cases were reported in 2014 globally; of these, 1.5 million died from the disease, and 5.7 million were newly diagnosed. Therefore, there is a strong need for fast and precise diagnostic methods, with higher sensitivity and specificity than existing assays.

At present, a diagnosis of active TB requires confirmed clinical samples from patients and is based on bacteriological methods, such as tuberculin skin tests (TSTs) and interferon gamma release assays (IGRAs) (Wu et al., 2014). These tests are limited by low specificity, low sensitivity, and costly reagents. TST is not an appropriate method to diagnose active TB,

as it only indicates whether the patient has been infected or not. Moreover, TST may provide false-positive and false-negative results in people who have been vaccinated with *Bacillus Calmette-Guerin*. Moreover, TST might give false-positive results for those who have been infected with TB in the past as their memory T cells still secrete interferon-γ. These methods are indirect measures of an induced immune reaction against antigen exposure by a recent infection and reinfection. Furthermore, TSTs and IGRAs cannot distinguish between latent TB, active TB, and complete recovery from TB. To overcome these shortcomings, we have focused on *M. tuberculosis* secretory proteins suitable for early detection of TB. One of these is Ag85B, a major secretory antigen from active *M. tuberculosis*.

The aim of this study was to use a combination of gold nanorods (AuNRs) and silica-coated quantum dots (SiQDs) to enhance the sensitivity of sandwich assays. AuNRs are excellent candidates for biosensors because they present an expandable visible spectrum and a larger surface area than gold nanoparticles (Nikoobakgt and El-Sayed, 2003; Sau and Murphy, 2004; Wang et al., 2010; Chen et al., 2011; Wang et al., 2011). Owing to their anisotropic rod shape, AuNRs are characterized by biocompatibility, chemical stability, and rapid electron transfer (Jorge et al., 2005; Vigderman et al., 2012; Vigderman and Zubarev, 2013; Huang et al., 2014). This makes them interesting for biomedical and plasmonic applications involving the study of nucleic acids, metal ions, amino acids, and proteins (Hu et al., 2006; Huang et al., 2008; 2009; Alkilany et al., 2012; Warren et al., 2012). Quantum dots (QDs) are small light-emitting particles of nanometer size. They represent a new class of fluorescent probes for biological and medical applications (Marcel et al., 1998; Sondi et al., 2000; Taylor et al., 2000; Mamedova and Kotov, 2001; Chan et al., 2002; Wang et al., 2002; Alivisatos, 2004; Pinaud et al., 2006). Compared with conventional organic dyes and fluorescent proteins, QDs have unique optical and electronic properties, such as high

luminosity, simultaneous excitation of different fluorescent colors, and high stability against photobleaching (Marcel et al., 1998; Wu et al., 2003). The silica-shell coated QD forms a hybrid material (Rogach et al., 2000; Gerion et al., 2001). The silica nanoparticles are of great interest for their dimensional similarity to biomolecules (e.g., DNA and proteins) and for applications in biological imaging and bioconjugation.

AuNRs have been used previously in fluorescence-based assays for biological analysis, mostly through fluorescence resonance energy transfer (FRET). Accordingly, the excitation energy of the donor (SiQDs) is transferred to an acceptor (AuNRs) through an induced-dipole/induced-dipole interaction. FRET technology is very convenient and can be applied routinely at a single-molecule detection level. In addition, FRET is very sensitive due to the short distance between donor and acceptor (Maxwell et al., 2002; Lee et al., 2008; Griffin et al., 2009). Previously, a recombinant antibody immobilized on AuNRs was conjugated to SiQDs-SiBP-8B3, whereby 8B3 was another TB secretory antibody. When this complex was bound to Ag85B, FRET between SiQDs and AuNRs was observed and the intensity of SiQDs red fluorescence decreased (Nie and Emory, 1997; Krug et al., 1999).

Herein, we studied the bioconjugation of AuNRs and SiQDs with proteins to create complex structures. We report the preparation of bioconjugates of antigen and antibody to AuNRs and SiQDs of different size. Moreover, we demonstrated that such immunocomplexes can be used to improve the detection of *M. tuberculosis* in a sandwich assay via antigen-antibody interactions using AuNRs and SiQDs. This can be accomplished by taking advantages of the competitive inhibition of FRET in antigen-antibody immunocomplexes (**Fig. 1**). We have developed a highly sensitive, selective, specific, fast and economical assay for the detection of TB secretory antigen in infected individuals. To this end, we employed

the secreted antigen Ag85B and fused recombinant antibodies GBP-50B14 and SiBP-8B3 for the detection of the active *M. tuberculosis*.

2. Materials and methods

2.1. Materials

Gold (III) chloride trihydrate ($HAuCl_4\ 3H_2O$), cadmium perchlorate hydrate ($Cd(ClO_4)_2$), sodium silicate ($Na_2O_7Si_3$), thioglycolic acid ($HSCH_2COOH$, TGA), bovine serum albumin (BSA), ampicillin, isopropyl-β-D-thiogalactopyranoside (IPTG) and phosphate-buffered saline (PBS, pH 7.4) were purchased from Sigma-Aldrich (St. Louis, MO, USA). L-ascorbic acid (99.5%) and hydrochloric acid (HCl) were from Samchun Chemical (Pyeongtaek, Korea). The secretory antigen, Ag85B, from *M. tuberculosis* was obtained from Chungnam National University (Daejeon, Korea). Cetyltrimethylammonium bromide (CTAB), sodium borohydride ($NaBH_4$), and silver nitrate ($AgNO_3$) were purchased from Daejung Chemicals (Siheung, Korea). Sulfuric acid (98%) was from Junsei (Tokyo, Japan). (3-mercaptopropyl)trimethoxysilane ($HS(CH_2)_3Si(OCH_3)_3$, MPS, 95%) was purchased from Alfa Aesar (Ward Hill, MA, USA). Spectra/Por dialysis membrane (6,000–8,000 kDa molecular weight cut-off) was supplied by Spectrum Labs (Rancho Dominguez, CA, USA). Aluminum telluride (Al_2Te_3) was purchased from Advanced Chemical Company (Warwick, RI, USA). Deionized (DI) water at 18.2 MΩ cm was purified using a Milli-Q system (Millipore, Billerica, MA, USA). All chemicals were used without further purification.

2.2. Synthesis of AuNRs

AuNRs were synthesized by a chemical reduction process using a seeding growth method as previously reported (Huang et al., 2014). Briefly, gold seed particles were prepared by mixing 5 mL of 0.5 mM $HAuCl_4$ with 5 mL of 0.2 M CTAB, followed by addition of 0.6 mL of 10 mM ice-cold $NaBH_4$ and vigorous stirring. The seed solution was prepared at least 2 h prior to use. For AuNR synthesis, 18 mL of 5 mM $HAuCl_4$ and 180 μL of 0.1 M $AgNO_3$ were added to 90 mL of 0.2 M CTAB. Upon addition of 180 μL of 1.2 M HCl and 10.5 mL of 10 mM ascorbic acid the mixture was gently stirred as the color turned from dark orange to transparent. After the color change, 150 μL CTAB-stabilized gold seed solution was rapidly injected, gently mixed for 10 s, and left undisturbed overnight at 37°C.

In order to change the size of AuNRs, we varied the seeding concentration of $AgNO_3$ (0.01–0.1 M in aqueous solution), since metal ions are important for the nanorod growth. To remove CTAB, the resulting solution was centrifuged three times at 15,110 × *g* for 10 min, and the pellet was resuspended in DI water. The color change of the resulting solution depended on the concentration of silver ions.

2.3. Synthesis of thiol-capped CdTe QDs and SiQDs

The aqueous synthesis of thiol-capped CdTe QDs followed previous reports (Gaponik et al., 2002; Rogach et al., 2007). Typically, 0.985 g (2.35 mM) $Cd(ClO_4)_2 \cdot 6H_2O$ was dissolved in 125 mL DI water inside a three-necked flask and 5.7 mM TGA, a thiol stabilizer, was added under stirring. To adjust the pH, 1.0 M NaOH was added drop by drop until a clear solution was obtained. TGA was replaced by CdTe nanocrystals by refluxing the reaction mixture at 100°C under stirring and open-air conditions with a condenser attached. The mixture was placed in a three-necked flask and was deaerated by N_2 bubbling for 20 min. The tellurium

precursor H_2Te was prepared by adding 15–20 mL of 0.5 M sulfuric acid dropwise to a 0.2 g (0.46 mM) lump of Al_2Te_3 under constant stirring, followed by N_2 bubbling for 20 min. The product was stored at 4°C.

To prepare SiQDs (Wolcott et al., 2006), 1.5 mL MPS (48 mM in pure ethanol) was added to a 10 mL solution of CdTe QDs. To produce a homogeneous dispersion of MPS, the mixture was stirred during the 2 h required for surface priming. Next, the solution was dialyzed against 2.0 L DI water for 1 h. In order to ensure whole surface coverage, an additional 1.5 mL MPS was added and continued dialysis for 1 h. After surface priming, 2 mL sodium silicate was added to the solution under stirring to begin silica polymerization around the surface of the particles. This was continued for 12 h to ensure shell growth around CdTe QDs. To potentialize silica shells, silicate solubility was decreased by addition of 2 mL ethanol followed by vortexing to ensure suitable mixing until the solution was slightly turbid. SiQDs were centrifuged at 15,110 × *g* for 2 min and the supernatant was discarded. The QD pellet was resuspended in 1 mL DI water and then sonicated for 30 min. In order to determine the concentration of SiQDs in solution, absorption spectrum method was used as described in a previous report (Yu et al., 2003).

2.4. Production of GBP-50B14 and SiBP-8B3 fusion protein

A codon-optimized GBP N-terminally fused 50B14 with a His-tag at its C-terminus was cloned into a pET-22b(+) vector and then transformed into *Escherichia coli* BL21(DE3) strain. Similarly, a codon-optimized SiBP N-terminally fused 8B3 with a His-tag at its C-terminus was cloned into a pET-22b(+) vector and then transformed into *E. coli* BL21(DE3) strain. A 100 µL of the *E. coli* BL21(DE3) harboring recombinant vector was incubated in 10

mL of Luria-Bertani (LB) medium containing 100 μg mL^{-1} for 16 h at 25°C with 200 rpm stirring rate. After incubation, 1 mL of the incubated *E. coli* solution was incubated again with a 100 mL of LB medium for 2 h for proliferation of the cells. Then, the cell concentration of the culture solution was measured by a UV/Vis spectroscopy. When the absorbance value at 600 nm, $OD_{600,}$ was reached at 0.4, 0.5 mM IPTG was added for induction of fusion protein. After further incubation for 7 h, the cells were centrifuged at 3,500 rpm for 10 min, and then cell pellet was obtained after removal of supernatant. This cell pellet was resuspended in phosphate-buffered saline solution and ultrasonicated then centrigued at 13,000 rpm to collect insoluble fraction of proteins. Expression of the GBP-50B14 (32.2 kDa) and SiBP-8B3 (29.1 kDa) was confirmed by sodium dodecyl sulfate polyacrylamide gel electrophoresis (SDS-PAGE, **Fig. S1**). The collected fusion protein was purified with an AKTA purifier (GE Healthcare Bio-Science, Piscataway, NJ, USA) using a Ni-column and stored at 4°C until used. The protein concentrations were determined by Bradford's method using BSA as a standard.

2.5. Surface plasmon resonance (SPR) analysis

To optimize the concentration of fused recombinant antibodies, GBP-50B14 and SiBP-8B3 for sandwich assay to Ag85B was verified by SPR analysis. Combinations of the fusion protein and specific antibodies against Ag85B were immobilized on the surface of a SPR gold chip and characterized using a BIAcore 3000^{TM} unit (GE Healthcare, Chicago, IL, USA) with an automatic flow injection system (Kim et al., 2015). All reagents were resuspended in 1X PBS (pH 7.4) and experiments were conducted at room temperature. A clear SPR sensor chip was attached to a separate chip carrier for easy assembly. After combination and priming

on the SPR chip, the activated surface was flushed with PBS to minimize non-specific binding of any unbound sites by removing slack bound material and foreign matter. This was achieved using a liquid handling micropipette in the SPR system. Gold binding polypeptide (GBP) was used as a model fusion protein for convenient protein immobilization onto the gold surface (Park et al., 2006; Yang et al., 2011). All SPR sensorgrams used BIA evaluation software (GE Healthcare). Concentrations of GBP-50B14 and SiBP-8B3 were optimized by continuous infusion of the bound state solution over the surface of the SPR gold chip, as described below.

For equilibration, 1X PBS (pH 7.4) was allowed to flow on the exposed gold chip surface for 10 min. Then, various concentrations (25, 50, 100, and 200 μg mL^{-1}) of GBP-50B14 were passed over the chip surface at a rate of 5 μL min^{-1}. Next, 10 μg mL^{-1} of Ag85B was flowed at 5 μL min^{-1}. The same flow rate was used for 50 μg mL^{-1} SiBP-8B3. Once optimum concentration of GBP-50B14 was fixed, the same procedure was carried out with different concentrations (25, 50, 100, and 200 μg mL^{-1}) of SiBP-8B3, respectively. Between the conjugations of each reagent, blocking step was carried out for 10 min with 500 μg mL^{-1} BSA to reduce non-specific binding.

The concentration of GBP-50B14 was fixed to 100 μg mL^{-1} as highest resonance unit (RU) of 2,643 was obtained at this concentration. Similarly, the concentration of SiBP-8B3 was fixed to 200 μg mL^{-1}. Finally, different concentrations (10, 20, 40, and 80 μg mL^{-1}) of Ag85B were analyzed under SPR to confirm optimized concentration of GBP-50B14 and SiBP-8B3, respectively (**Fig. S2**).

2.6. Conjugation

2.6.1. Conjugation of AuNRs-GBP-50B14

Briefly, 100 μL AuNRs was mixed with 100 μL of 400 μg mL^{-1} GBP-50B14 and incubated at 37°C for 30 min with shaking. Unbound antibody was washed out by centrifugations at 15,110 × *g* for 10 min. AuNRs-GBP-50B14 conjugates were resuspended in 200 μL PBS and stored at 4°C.

2.6.2. Conjugation of SiQDs-SiBP-8B3

Silica-binding polypeptide (SiBP) was used as a model protein for direct immobilization onto the silica surface (Gu et al., 2009; Ahn et al., 2012; Kim et al., 2014). Briefly, 100 μL SiQDs was mixed with 100 μL of 400 μg mL^{-1} SiBP-8B3 and incubated at 37°C for 30 min with shaking. Next, 20 μL 10% (w/v) casein, a blocking agent, was added and the mixture was incubated overnight. Unbound samples were removed through centrifugations at 15,110 × *g* for 10 min. SiQDs-SiBP-8B3 conjugates were resuspended in 200 μL PBS and stored at 4°C.

2.7. Characterization

UV-vis absorption spectra of aqueous sample solutions were obtained using Optizen POP (Mecasys, Daejeon, Korea). Micrographs and X-ray energy dispersive spectroscopy (EDS) elemental analyses were obtained using a Field Emission transmission electron microscope (FE-TEM; model TECNAI G2 F30 S-Twin, FEI, OR, USA) operated at an acceleration voltage of 300 keV. Lattice constants were also measured with a high-resolution transmission electron microscope (HR-TEM, 300 kV, JEM-3010, Jeol, Tokyo,

Japan). The preparation of TEM grids was as follows. Typically, 1.5 mL of the solution was centrifuged for 10 min at 15,110 × *g* to precipitate the solid phase. The colorless supernatant was discarded, while the solid residue was resuspended in 1.5 mL DI water and centrifuged again. A total 20 μL of this solution was dropped on the TEM grid and allowed to dry in open air. To visualize the shape and the surface modifications of synthesized particles, a field-emission scanning electron microscope (FE-SEM, S-4800, Hitachi, Tokyo, Japan) was used. Structural functional groups were analyzed by Fourier transform infrared spectroscopy (FT-IR, IFS6v/S, Bruker, Karlsruhe, Germany). Fluorescence of SiQDs was measured by using a multi-mode microplate reader (BioTek Synergy H1, Winooski, VT, USA) with black polystyrene 96-well microplate.

3. Results and discussion

3.1. Characterization of nanomaterials and functionalizations

3.1.1. Synthesis of AuNRs controlled by $AgNO_3$ and conjugation of primary antibody

UV-vis absorption spectra of AuNRs are shown in **Fig. 2a**. Application of a small amount of $AgNO_3$ was reported to have an enormous effect on rod yield and dimensions (Brown et al., 2000). With the proper ratio of the seed to gold ion concentrations and addition of an appropriate quantity of $AgNO_3$, we obtained a high yield (~97%) of rod-shaped particles. Aspect ratio of the AuNRs could be increased up to 3.8 times by raising the concentration of $AgNO_3$. CTAB-coating over AuNRs worked as a bilayer, preventing aggregation and allowing its growth by face-sensitive surface adsorption. Visible-near infrared absorption spectra also revealed that the rod yield in the absence of $AgNO_3$ was considerably lower, as

shown by the relative values of longitudinal plasmon absorbance. Presence of $AgNO_3$ in the growth solution led to a longitudinal plasmon absorbance peak **(Fig. S3)**. Different aspect ratios were obtained by varying the concentration of $AgNO_3$ from 0.01 to 0.1 M. However, AuNRs were not synthesized when the concentration of $AgNO_3$ was below 0.02 M (**Fig. S3a**). The presence of gold (Au) in synthesized AuNRs was confirmed by energy-dispersive spectroscopy (EDS) (**Fig. S3c**). The different aspect ratios were confirmed by absorption spectra (**Fig. S3b**), their colors (**Fig. S3d**), and TEM images (**Fig. S3e–S3n**). Au^{3+} ions decreased when acid (HCl) was added to the growth solution, facilitating the formation of AuNRs with large aspect ratios. An increase in $AgNO_3$ produced a red shift in the absorption spectra, indicating a different length of AuNRs.

The synthesized AuNRs were conjugated with recombinant antibody 50B14 fused to GBP as a novel immunoassay probe. GBPs have been widely employed onto gold surfaces as linkers for protein immobilization and the development of biosensing devices. In this case, the GBP {111} was fused to the N-terminus of 50B14 (Braun et al., 2002; Sarikaya et al., 2003). Although binding of GBP and thiol to the gold surface is similar, the level of Gibbs-free energy of the former makes it more stable (Tamerler et al., 2006). This suggests that the strong binding of GBP onto the gold particle does not require any additional surface modification. The GBP-50B14 antibody attached onto the surface of AuNRs and the F_{ab} domain of the gold-labeled probe interacted with the surface of the Ag85B antigen. Conjugation of AuNRs with GBP-50B14 was confirmed by a 10-nm shift in UV-vis absorption spectra (**Fig. 2b**).

3.1.2. Synthesis of SiQDs and conjugation of secondary antibody

Encapsulated in a silica shell of about 15 nm, QDs surface was functionalized with amine groups. Silica-coated (or silanized) nanocrystals were soluble in buffer solutions over a wide pH range even at high salt concentrations (up to 200 mM), retaining the optical properties of the original core/shell particles. Moreover, silica-coated nanocrystals were more stable in biological buffers than nanoparticles primed with thiolated molecules such as mercaptopropionic acid. SiQDs fluorescence spectra revealed an emission peak at 630 nm (**Fig. 3a** and **Fig. S4a**), while TEM images indicated a 3.5 nm average size (**Fig. 3c**). **Fig. S4b** presents FT-IR spectra of silica-coated and -uncoated CdTe QDs. The characteristic peaks of CdTe QDs (uncoated) revealed an asymmetric stretching vibration of the carboxyl group (1636 cm^{-1}), indicating the presence of organic COO^- groups on the surface of CdTe particles. In addition, a thiol stretching vibration (2117 cm^{-1}), which was clearly present in pure TGA, was absent in the spectra of SiQDs. This implies that the thiol group of TGA has been attached to the surface of QDs through a strong Cd-S bond. The absorption peaks of SiQDs attributed to asymmetric Si-O-Si stretching (1234 cm^{-1}) and Si-O-Si bending (903 cm^{-1}), confirming the formation of the silica shell. The presence of silica (Si), cadmium (Cd) and telluride (Te) was confirmed by energy-dispersive spectroscopy (EDS) (**Fig. S4c**).

The synthesized SiQDs were conjugated with SiBP-8B3 since it binds well to silica surfaces (Taniguchi et al., 2007; Kacar et al., 2009). SiBP can be used for biosensing without any surface modification or self-assembled monolayer (Kacar et al., 2009). When SiBP-8B3 was attached to the surface of SiQDs in PBS at 37°C for 30 min, a 5-nm shift in the fluorescence peak was observed due to the screening effect of SiBP-8B3 (**Fig. 3a)**. SiQDs were employed in this study because of their simple conjugation onto SiBP-8B3, which showed a strong quenching effect after injection of Ag85B antigen due to the short distance between the two complexes formed by sandwich interaction with Ag85B for 30 min at 37°C.

This was confirmed by a 10-nm shift to the right, suggesting that the sandwich assay could be applied for the TB antigen detection. In addition, potential application of the sandwich assay was also confirmed through TEM image showing AuNRs-Ag85B-SiQDs complex (**Fig. 3d**).

3.2. Optimization of detection conditions

Based on the sandwich assay, GBP-50B14 antibody was conjugated onto the surface of differently sized AuNRs. As more antibodies can be attached to a larger AuNR, optimum concentration of $AgNO_3$ was chosen as 90 mM according to absorption spectra and Bradford assay (**Fig. S5**). SiQDs concentration was optimized in the range of 2–8 μM. As shown in **Fig. S6**, conjugation efficiency of SiBP-8B3 was highest at 6 μM SiQDs.

In order to reduce non-specific binding, we used BSA (1% w/v) and casein (1% w/v) as blocking reagents. In the case of AuNRs, absorption spectra, SDS-PAGE, and quantitative analysis showed a relatively small benefit of blocking (**Fig. S7a**). Therefore, blocking reagent was not used in the conjugation of AuNRs with GBP-50B14.

In contrast, blocking step made a difference in SiQDs experiments. There was a great decrease in fluorescence intensity after the addition of blocking reagents compared to before (**Fig. S7b**). This indicates that blocking reagents successfully blocked non-specific binding sites on the surface of SiQDs. As casein proved to be more effective than BSA, casein was used as a blocking reagent in conjugation of SiQDs with SiBP-8B3.

3.3. Sensitivity of Ag85B detection

We evaluated the fluorescence sensitivity of the developed sandwich assay using SiQDs

and AuNRs. Under optimum conditions, a good inverse linear relationship between fluorescence intensity and the concentration of Ag85B was obtained (**Fig. 4**). At high Ag85B concentrations, the distance between AuNRs and SiQDs got closer and thus fluorescence decreased through FRET. The linear range was from 1×10^{-3} to 1×10^{-10} μg mL^{-1} ($R^2 = 0.974$) with a limit of detection (LOD) for Ag85B as low as 13.0 pg mL^{-1}. The developed sandwich assay shows lower LOD than most of the reported research except for PCR analysis (**Table 1**). Although PCR method shows high sensitivity, its major disadvantages such as DNA preparation and complicated procedures cannot be avoided. Thus, direct detection of Ag85B through the developed sandwich assay can be used for better diagnosis of TB.

3.4. Specificity and selectivity of Ag85B detection

To verify the specificity of this assay, we tested the system with two possible interfering compounds, BSA and CFP10 - another secreted antigen of *M. tuberculosis* (Kim et al., 2013). The concentration of Ag85B, CFP10, and BSA used in the assay was 10 μg mL^{-1}. As shown in **Fig. 5**, the fluorescence intensities for BSA and CFP10 are roughly the same with the control, while Ag85B resulted a tremendous decrease in fluorescence intensity. These results suggest that the developed sandwich assay displays excellent specificity to Ag85B based on FRET.

3.5. Sandwich detection of Ag85B in spiked and real samples

For further application of the developed sandwich assay, we prepared a batch of urine extracts with varying concentrations of Ag85B. Three different spiked urine samples from

three volunteers were assayed for recovery. A summary of the spiked sample concentrations and results of corresponding analysis are shown in **Table 2**. The results showed that recoveries were in the range of 92–104% with relative standard deviations of 6–37% confirming successful detection of Ag85B in complex samples.

4. Conclusion

In summary, we have demonstrated that silica-coated red-fluorescent CdTe QDs with AuNRs bound to a GBP-fused antibody probe can be applied in the detection of Ag85B, secreted antigen of *M. tuberculosis* based on FRET. AuNRs were used as an optimal quencher for fluorescence quenching of QDs, and QDs were coated with silica for easy binding with SiBP-fused antibody. This sandwich assay showed excellent fluorescence quenching effect in the presence of the target, Ag85B with the detection limit of 13 pg mL^{-1}. High sensitivity of the sandwich assay was also confirmed by high recovery from spiked test. The easy preparation of nanomaterials and sensitive detection of Ag85B showed potential application in real samples. To the best of our knowledge, this is the first report using two recombinant antibodies conjugated with AuNRs and SiQDs for detecting TB secretory antigen, Ag85B. Furthermore, the developed sandwich assay based on FRET is not only simple, sensitive, and specific but can also be widely used for detection of many antigens secreted from pathogens including *M. tuberculosis*.

Acknowledgments

This work was supported by a grant from the Korean Health Technology R&D Project, Ministry of Health & Welfare, Republic of Korea (HI13C0862; HI16C1553).

Appendix A. Supplementary information

Supplementary data associated with this article can be found in the online version at http://dx.doi.org/10.1016/j.bios.2016.xx.xxx.

References

Ahn, J.-H., Kim, J.-Y., Choi, K., Kim, D.-I., Kim, C.-H., Seol, M.-L., Park, T.J., Lee, S.Y., Choi, Y.-K., 2012. IEEE Transact. Electron. Dev. 59, 2243-2249.

Alivisatos, P., 2004. Nat. Biotechnol. 22, 47-52.

Alkilany, A.M., Thompson, L.B., Boulos, S.P., Sisco, P.N., Murphy, C.J., 2012. Adv. Drug Deliv. Rev. 64, 190-199.

Braun, R., Sarikaya, M., Schulten, K.S., 2002. J. Biomater. Sci. Polym. E 13, 747–758.

Brown, K.R., Walter, D.G., Natan, M.J., 2000. Chem. Mater. 12, 306-313.

Chan, W.C.W., Maxwell, D.J., Gao, X., Bailey, R.E., Han, M., Nie, S., 2002. Curr. Opin. Biotechnol. 13, 40-46.

Chen, G., Jin, Y., Wang, L., Deng, J., Zhang, C., 2011. Chem. Commun. 47, 12500-12502.

Gaponik, N., Talapin, D.V., Rogach, A.L., Hoppe, K., Schevchenko, E.V., Kornowski, A., eychmiiller, A., Weller, H., 2002. J. Phys. Chem. B 106, 7177-7185.

Gerion, D., Pinaud, F., Williams, S.C., Parak, W.J., Zanchet, D., Weiss, S., Paul, A., 2001. J. Phys. Chem. B 105, 8861-8871.

Griffin, J., Singh, A.K., Senapati, D., Rhodes, P., Mitchell, K., Robinson, B., Yu, E., Ray,

P.C., 2009. Chem. Eur. J. 15, 342-351.

Gu, B., Park, T.J., Ahn, J.-H., Huang, X.-J., Lee, S.Y., Choi, Y.-K., 2009. Small 5, 2407-2412.

Hu, M., Chen, J., Li, Z.Y., Au, L., Hartland, G.V., Li, X., Marquez, M., Xia, Y., 2006. Chem. Soc. Rev. 35, 1084-1094.

Huang, H., Wang, J.H., Jin,W., Li, P., Chen, M., Xie, H.H., Yu, X.F., Wang, H., Dai, Z., Xiao, X., Chu, P.K., 2014. Small 10, 4012-4019.

Huang, X., Jain, P.K., El-Sayed, I.H., El-Sayed, M.A., 2008. Lasers Med. Sci. 23, 217-228.

Huang, X., Neretina, S., El-Sayed, M.A., 2009. Adv. Mater. 21, 4880-4910.

Jorge, P.-J., Isabel, P.-S., Luis, M.L.-M., Paul, M., 2005. Coord. Chem. Rev. 249, 1870-1901.

Kacar, T., Ray, J., Gungormus, M., Oren, E.E., Tamerler, C., Sarikaya, M., 2009. Adv. Mater. 21, 295-299.

Kim, J., Lee, J., Lee, K.I., Park, T.J., Kim, H.J., Lee, J., 2013. Sensor. Actuat. B-Chem. 177, 327-333.

Kim, J., Hong, S.C., Hong, J.C., Chang, C.L., Park, T.J., Kim, H.J., Lee, J., 2015. Sensor. Actuat. B-Chem. 216, 184-191.

Kim, J.-Y., Ahn, J.-H., Moon, D.-I., Park, T.J., Lee, S.Y., Choi, Y.-K., 2014. Biosens. Bioelectron. 55, 162-167.

Kim, G.W., Kim, M.S., Park, T.J., 2015. Biosens. Bioelectron. 67, 408-412.

Krug, J.T., Wang, G.D., Emory, S.R., Nie, S., 1999. J. Am. Chem. Soc. 121, 9208-9214.

Lee, S., Cha, E.J., Park, K., Lee, S.Y., Hong, J.K., Sun, I.C., Kim, S.Y., Choi, K., Kwon, I.C., Kim, K., Ahn, C.H., 2008. Angew. Chem. Int. Ed. 120, 2846-2849.

Mamedova, N.N, Kotov, N.A., 2001. Nano Lett. 1, 281-286.

Marcel, B.J., Moronne, M., Gin, P., Weiss, S., Paul, A.A., 1998. Science 281, 2013-2015.

Maxwell, D.J., Taylor, J.R., Nie, S., 2002. J. Am. Chem. Soc. 124, 9606-9612.

Nie, S., Emory, S.R., 1997. Science 275, 1102-1106.

Nikoobakgt, B., El-Sayed, M.A., 2003. Chem. Mater. 15, 1957-1962.

Park, T.J., Lee, S.Y., Lee, S.J., Park, J.P., Yang, K.S., Lee, K.-B., Ko, S., Park, J.B., Kim, T., Kim, S.K., Shin, Y.B., Chung, B.H., Ku, S.-J., Kim, D. H., Choi, I.S., 2006. Anal. Chem., 78, 7197-7205.

Phunpae, P., Chanwong, S., Tayapiwatana, C., Apiratmateekul, N., Makeudom, A., Kasinrerk W., 2014. Diagn. Micr. Infec. Dis. 78, 242-248.

Pinaud, F., Michalet, X., Bentolila, L.A., Tsay, J.M., Doose, S., Li, J.J., Iyer, G., Weiss, S., 2006. Biomaterials 27, 1679-1687.

Rogach, A.L., Dattatri, N., Ostrander, J.W., Michael, G., Nicholas, A.K., 2000. Chem. Mater. 12, 2676-2685.

Rogach, A.L., Thomas, F., Klar, T.A., Feldmann, G., Gaponik, N., Lesnyak, V., Shavel, A., Eychmiiller, A., Rakovich, Y.P., Donegan, J.F., 2007. J. Phys. Chem. B 111, 14628-14637.

Saengdee, P., Chaisriratanakul, W., Bunjongpru, W., Sripumkhai, W., Srisuwan, A., Hruanun, C., Poyai, A., Phunpae, P., Pata, S., Jeamsaksiri, W., Kasinreak, W., Promptmas, C., 2016. Analyst http://dx.doi.org/10.1039/C6AN00568C.

Sarikaya, M., Tamerler, C., Jen, A.K., Schulten, K., Baneyx, F., 2003. Nat. Mater. 2, 577–585.

Sau, T.K., Murphy, C.J., 2004. Langmuir 20, 6414-6420.

Singh, N., Sreenivas, V., Gupta, K.B., Chaudhary, A., Mittal, A., Varma-Basil, M., Prasad, R., Gakhar, S.K., Khuller, G.K., Mehta, P.K., 2015, Diagn. Micr. Infec. Dis. 83, 359-

364.

Sondi, I., Siiman, O., Koester, S., Matijevic, E., 2000. Langmuir 16, 3107-3118.

Tamerler, C., Duman, M., Oren, E.E., Gungormus, M., Xiong, X., Kacar, T., Parviz, B.A., Sarikaya, M., 2006. Small 2, 1372–1378.

Taniguchi, K., Nomura, K., Hata, Y., Nishimura, T., Asami, Y., Kuroda, A., 2007. Biotechnol. Bioeng. 96, 1023–1029.

Taylor, J.R., Fang, M.M., Nie, S., 2000. Anal. Chem. 2000, 1979-1986.

Vigderman, L., Khanal, B.P., Zubarev, E.R., 2012. Adv. Mater. 24, 4811-4841.

Vigderman, L., Zubarev, E.R., 2013. Chem. Mater. 25, 1450-1457.

Wang, S.H., Lee, C.W., Chiou, A., Wei, P.K., 2010. J. Nanobiotechnol. 8, 33.

Wang, L., Jin, Y., Deng, J., Chen, G., 2011. Analyst 136, 5169-5174.

Wang, S., Mamedova, N., Kotov, N.A., Chen, W., Studer, J., 2002. Nano Lett. 2, 817-822.

Warren, S.C., Thimsen, E., 2012. Energy Environ. Sci. 5, 5133-5146.

Wolcott, A., Gerion, d., Visconte, M., Sun, J., Schwartzberg, A., chen, S., Zhang, J.Z., 2006. J. Phys. Chem. B 110, 5779-5789.

Wu, H.-J., Li, Y., Fan, J., Deng, Z., Hu, Z., Liu, X., Graviss, E.A., Reffari, M., Ma, X., Hu, Y., 2014. Anal. Chem. 86, 1988-1996.

Wu, X., Liu, H., Liu, J., Haley, K,N., Treadwas, J.A., Larson, J.P., Ge, N., Peale, F., Bruchez, M.P., 2003. Nat. Biotechnol. 21, 41-46.

Yang, M., Choi, B.G., Park, T.J., Heo, N.S., Hong, W.H., Lee, S.Y., 2011. Nanoscale 3, 2950-2956.

Yu, W. W., Qu, L., Guo, W., Peng, X., 2003. Chem. Mater. 15, 2854-2860.

Fig. 1. Schematic illustration of a novel fluorescent analysis method for the detection of secreted antigen from *M. tuberculosis* based on sandwich assay *via* antigen-antibody interaction using AuNRs and SiQDs.

Fig. 2. (a) UV-vis absorption spectra of GBP-50B14 (red line) conjugation on the surface of AuNRs (black line). (b) TEM images of AuNRs.

Fig. 3. (a) Fluorescence spectrum of SiQDs (red line), SiBP-8B3 antibody-conjugated SiQDs (blue line) and AuNRs-Ag85B-SiQDs complex (black line) at excitation wavelength of 350 nm. (b) HRTEM image of CdTe QDs with extracted in-plane lattice constants. Average size of CdTe QDs is 3.5 nm. TEM images of (c) SiQDs and (d) AuNRs-Ag85B-SiQDs complex.

Fig. 4. Calibration curve of the sandwich assay for the detection of Ag85B; error bars were obtained from three parallel experiments. Graphs are linearized version of the curve by log transformation. LOD obtained from sandwich assay was 13.0 pg mL^{-1}.

Fig. 5. Fluorescence intensities of the sandwich assay used for the detection of Ag85B. Selectivity was determined by detecting Ag85B, CFP10 and BSA.

Table 1. Comparison of different assays for secretory antigens of *M. tuberculosis*

Target	Technique	Detection range (ng mL^{-1})	LOD (ng mL^{-1})	Reference
Ag85B	Sandwich ELISA	8 ~ 400	8	Phunpae et al., 2014
	Indirect ELISA	-	10	Singh et al., 2015
	Indirect sandwich ELISA	-	1	
	Indirect I-PCR	-	0.00001	
	Indirect sandwich I-PCR	-	0.000001	
	Silicon nitride ISFET	120 ~ 1000	120	Saengdee et al., 2016
	Sandwich ELISA	0.013 ~ 1	0.013	**This work**
CFP10	Magnetophoretic immunoassay	0.01 ~ 10	0.01	Kim et al., 2013
	BLI assay II : indirect immobilization	-	1000	Kim et al., 2015
	BLI assay III : indirect immobilization	-	10	

Table 2. Assay results summarizing Ag85B detection in spiked samples

Sample	Concentration of Ag85B ($\mu g\ mL^{-1}$)*	Measured Ag85B in samples ($\mu g\ mL^{-1}$) ± SD*	Recovery (%), n = 5
1	-7	-6.45 ± 2.61	92.2
2	-8	-8.19 ± 0.56	102.5
3	-9	-9.41 ± 1.14	104.5
4	-10	-10.27 ± 0.64	102.3

*The concentrations of Ag85B were calculated by Log with standard deviation (SD).

Highlights

- Fluorescence quenching detection system using quantum dots and gold nanorods.
- Sandwich Ag-Ab interaction to detect active Tuberculosis (TB) antigen.
- Sensitive detection of secretory antigen, Ag85B, from *Mycobacterium tuberculosis*.
- The limit of TB detection was 13 pg mL^{-1} within 1-hour in patient urine samples.